

Cooling curves and graphite shapes of eutectic temperature region in gray cast iron

Taiki Tsuchiya¹, Katsutoshi Shigeno¹, Hirokazu Kawashima¹ and Kenji Matsuda²

¹ Matsubara co., Ltd.

² UNIVERSITY OF TOYAMA

Graphite shape is important to consider mechanical property in gray cast iron. Chemical composition and cooling rate affect graphite morphology.

In this work, the column-shaped castings having various volumes were used to measure cooling curves. Cooling curves were related to microstructure.

Keywords: graphite shape. cooling curve, casting simulation

1. Introduction

Graphite shape is important to consider mechanical property in gray cast iron. Chemical composition and cooling rate affect graphite morphology [1,2]. Graphite morphology in gray cast iron has been distinguished from A-type to E-type by ASTM [3].

In gray cast iron, inverse chill and D-type graphite caused by rapid cooling are observed at the final solidification part or thick part, both of which solidifies the most slowly.

We showed that inverse chill and D-type graphite form due to rapid cooling from eutectic temperature range (γ -Fe+G+L) with the experimental and simulated result of our previous work [4,5].

In this work, the column-shaped castings having two different volumes were used to measure cooling curves. We measured cooling curves at the center region and the other regions.

B-type graphite has been observed near the surface, but the mechanism of formation B-type graphite has not been clarified. We will also show simulated cooling curves of forming B-type graphite.

2. Experimental procedure

The melt tapped from cupola having ability to melt 8t/hr was held in forehearth for 10 minutes. Later the melt was transferred to a ladle with carbon inoculant. The melt corresponding to FC250 gray cast iron was poured to mold having two different shaped cavity.

Fig.1 shows the molds in this work. One is shell cup mold having $\phi 30$ column-shaped cavity (Fig.1 a), the other is CO₂ mold having $\phi 50$ column-shaped cavity

(Fig.1 b). We called the castings from two molds $\phi 30$ shell cup cast and $\phi 50$ CO₂ cast, respectively.

The cooling curves were measured from the center to near the surface. In $\phi 30$ shell cup cast, they were measured at P1 and P2. In $\phi 50$ CO₂ cast, they were measured at P1, P2 and P3.

Casting simulation (ADSTEFAN) was used to study metal flow and solidification process.

Microstructures were observed with optical microscope. The matrixes were observed after etching with 3% nital.

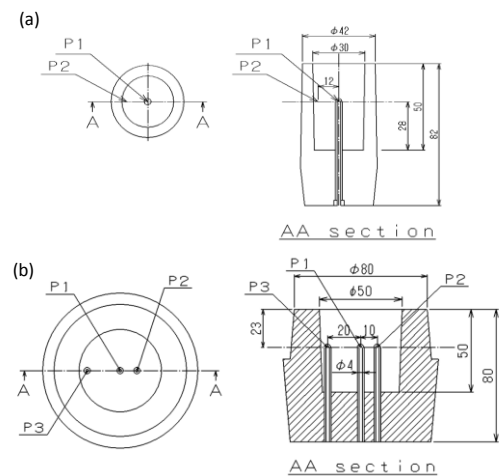


Fig.1 The molds in this work (a) $\phi 30$ shell cup cast, (b) $\phi 50$ CO₂ cast

3. Results and discussion

3.1 Cooling curves

Fig.2 shows the cooling curves in both of the castings. We could measure the cooling curves from center region to near the surface. The temperature at near the surface in both of castings were lower than center region.

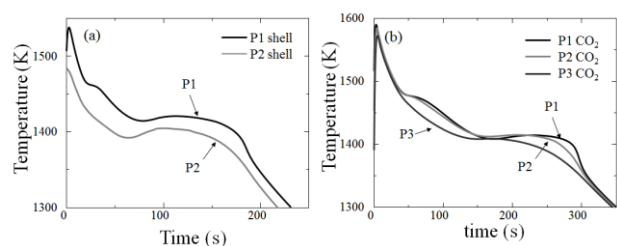


Fig.2 Cooling curves (a) $\phi 30$ shell cup, (b) $\phi 50$ CO₂ cast

3.2 Casting simulation

In casting simulation, the latent heat emission patterns were determined by the relationship between temperature and solid fraction. In our previous work, we recommended to use the model that has a certain temperature range in the solidification in accordance with Fe-C-Si ternary equilibrium phase diagram [5]. In this work, the temperature of primary crystal and eutectic were set from experimental values. In this simulation, three different temperature ranges for eutectic reaction were designated as follows :

1) The case of 1K

According to Fe-C binary equilibrium phase diagram, the eutectic temperature is constant. Therefore, the temperature of eutectic reaction end was set on 1420K for $\phi 30$ shell cup cast and 1414K for $\phi 50$ CO₂ cast.

2) The case of 10K

According to Fe-C-Si ternary equilibrium phase diagram [4], Si content may establish the eutectic temperature range. Therefore, the temperature of eutectic reaction end was set on 1411K and 1405K.

3) The case of 20K

We consider that the castings are multicomponent systems. Contents of P, Mn S, etc. may expand the temperature range. Therefore, the temperature of eutectic reaction end was set on 1401K and 1395K.

Fig.3 shows the results of casting simulation. The upper charts show the simulation results of $\phi 30$ shell cup cast in accordance with the three different temperature ranges described above. The bottom charts show the results of $\phi 50$ CO₂ cast. In the case of 1K, the simulated curves were different from experimental result. In the case of 10K, The difference between experiment and simulation became smaller than the case of 1K. In the case of 20K, the simulation closed to experiment in both of castings.

At P1 in both of castings, D-type graphite caused by rapid cooling and A-type graphite were observed. According to the experimental and simulation results, rapid cooling was observed at final solidification part. Therefore, it influenced formation of D-type graphite at P1. As previous work suggests [5], we show that the temperature of eutectic has temperature range (γ -Fe+G+L) and rapid cooling occurs at final solidification part with the experimental and simulated result.

Fig.4 shows microstructures near the surface in both of castings. B-type graphite was observed. The matrix near the B-type graphite was ferrite. We consider that the formation of B-type graphite occurred due to rapid

cooling around 50s in cooling curve at P2.

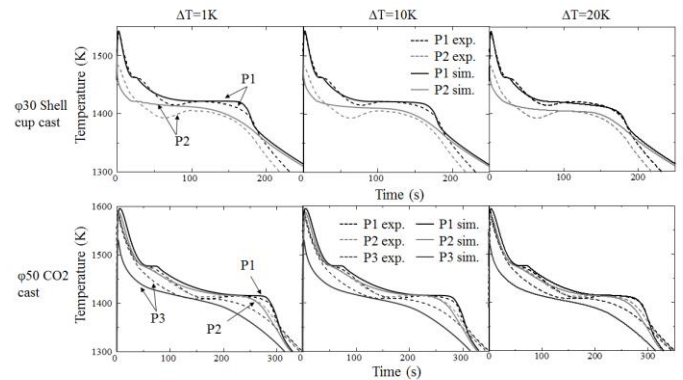


Fig.3 Simulation results of cooling curves with different eutectic temperature ranges

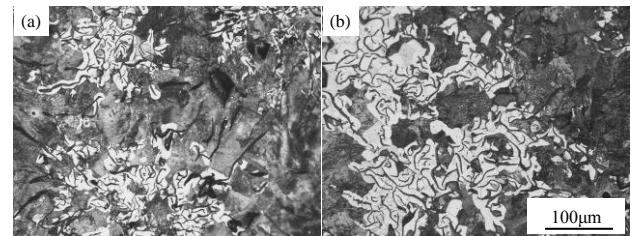


Fig.4 Microstructure near the surface in both of castings (a) $\phi 30$ shell cup, (b) $\phi 50$ CO₂ cast

4. Conclusions

We have done researches on the solidification in gray cast iron. The conclusions are as follows:

Through the measuring cooling curve and casting simulations, it was deduced the formation of D-type graphite occurred due to the rapid cooling at final solidification part.

On the other hand, the formation of B-type graphite near the surface occurred due to the rapid cooling observed in early stage of solidification.

References

- [1] H.Nakae, H.Shin, N.Hashihara: J.JFS 83 (1997) 562-569.
- [2] M.Makimura, K.Sakai, Y.Nishiyama, M.Tanaka: J.JFS 56 (1984) 15-21.
- [3] American Society for Metals: *Metals Handbook-Properties and Selection: Iron and steels-, 9th Ed. Vol.1*, (American Society of Metals, Metals Park, 1978) pp.13
- [4] American Society for Metals: *Metals Handbook-Properties and Selection: Iron and steels-, 9th Ed. Vol.1*, (American Society of Metals, Metals Park, 1978) pp.4
- [5] H.Kawashima, K.Shigeno, K.Tachibana : J.JFS 83 (2011) 3-6.